
Photooxidative Vulnerability to Intralipid in Photodynamic Therapy

Andrés M. Durantini,^{a-c*} Prabhu P. Mohapatra^a, Mommina Ashaque,^a Michael E. Zatoulovski,^a Michele M. Kim,^d Keith A. Cengel,^d Theresa M. Busch,^d Timothy C. Zhu,^d and Alexander Greer^{a,b*}

This chapter is intended to help make inroads to the role of Intralipid in photodynamic therapy (PDT). In addition to Intralipid's favorable property as a light scattering agent, we hypothesized that it will be unstable to photosensitized oxidation. To explore this, measurements of total quenching rate constants (k_T) of singlet oxygen with Intralipid and its constituents are described. Furthermore, organic phosphines were tested to trap Intralipid peroxides formed in photosensitized oxidation reactions. Our findings indicate that the vulnerability of Intralipid to photooxidation might suggest limits of its use in PDT.

1 Introduction

Intralipid is often used in photodynamic therapy (PDT).^{1,2} This is mainly due to Intralipid's useful light scattering properties with illumination by laser light. However, even with this property achieved, some of the Intralipid molecules may be decomposed and photoaged affecting their use in PDT. Here, we describe singlet oxygen ($^1\text{O}_2$) quenching by Intralipid and Intralipid peroxide trapping reactions that we think will be of interest to the fields of PDT, lipid oxidation, and even organic photochemistry.

The possible photoaging of Intralipid is caused by the unsaturated groups present in the liquid. Intralipid's composition is rich in unsaturated fatty acids. Intralipid contains soybean oil, egg yolk phospholipids, glycerol, and water (Fig. 1). Soybean oil itself consists of unsaturated fatty acids (oleic acid, linoleic acid, and linolenic acid) and saturated fatty acids (palmitic acid and stearic acid). The unsaturated fatty acids in Intralipid are particularly prone to oxidation by reactive oxygen species (ROS). ROS can be generated through a type I and type II photosensitized oxidation.^{3,4} In type I, the excited sensitizer can transfer an electron to form radicals that can later interact with oxygen to generate ROS such as hydroxyl radical (HO^\bullet), peroxy radical (ROO^\bullet), alkoxy radical (RO^\bullet), superoxide radical anion ($\text{O}_2^{\bullet-}$), and hydrogen peroxide (H_2O_2). In type II, the excited sensitizer transfers energy to $^3\text{O}_2$ to produce $^1\text{O}_2$, as the main cytotoxic species.⁵⁻⁸ Girotti et al.⁹ discuss this facet in lipids where type I (oxygen radicals) and type II ($^1\text{O}_2$) sensitized oxidation leads to oxygen radicals and radical ions, and singlet oxygen, which are trapped by fatty acids (Fig. 2). Girotti's experiments revealed discernible contributions from type I and type II sensitized oxidation.⁹ Allylic H abstraction and double-bond shift are characteristic of the $^1\text{O}_2$ 'ene' (type II) reaction.¹⁰⁻¹⁴ By contrast, oxygen radical H abstraction leads to the pentadienyl radical, thereby adding ground-state molecular oxygen ($^3\text{O}_2$) only to the 9' and 13' sites.⁹

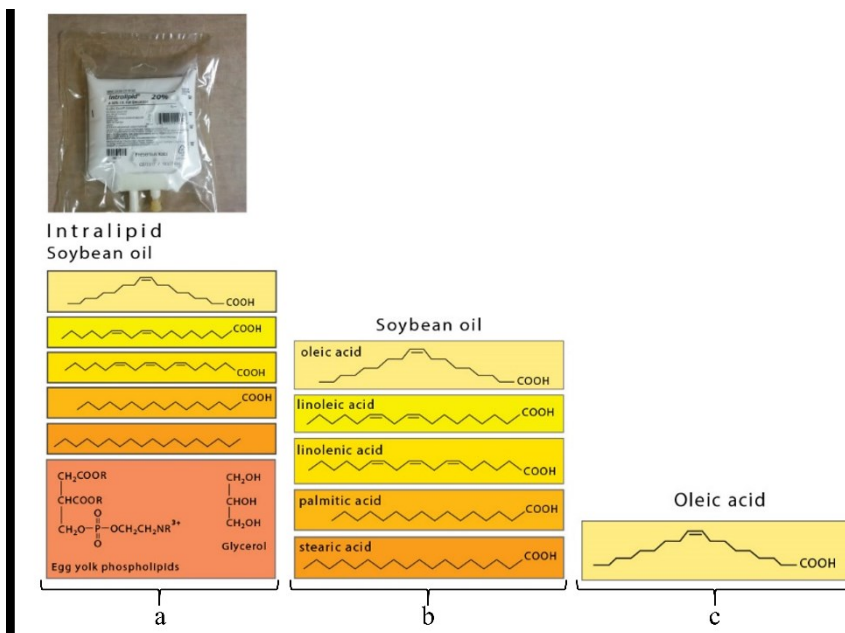
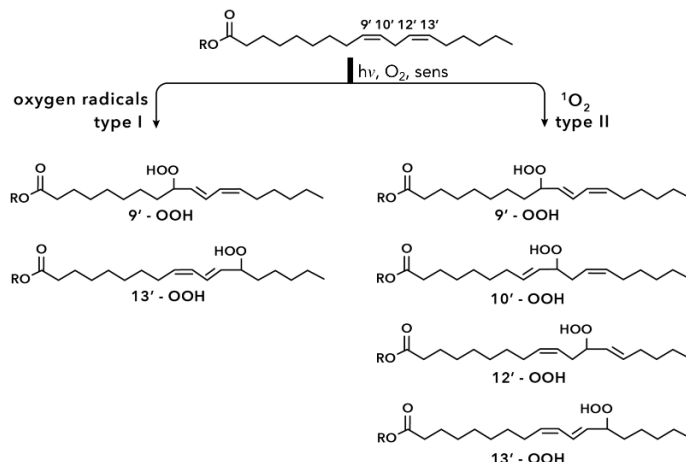


Fig. 1 Reagents used in this report: (a) Intralipid which consists of soybean oil, egg yolk phospholipids, and glycerol, (b) soybean oil which consists of oleic acid, linoleic acid, linolenic acid, palmitic acid and stearic acid, and (c) oleic acid. Soybean oil and oleic acid are used as simpler



“model” reactions in place of Intralipid.

Fig. 2 Type I (oxygen radicals) and type II (${}^1\text{O}_2$) sensitized oxidation of an unsaturated fatty acid and resultant hydroperoxide products.

It is worth knowing when Intralipid is likely to trap ROS in type I and type II sensitized oxidation due to its use in PDT. In pleural PDT, treatment is suitable for localized tumors such as those in malignant pleural mesothelioma (MPM).^{15,16} In a phase II study, the sensitizer Photofrin® is administered 24 hours before surgery at a dosage of 2 mg/kg, after which a large mass of the tumor is removed and followed

up by the addition of Intralipid (0.01%). Then the PDT treatment lasts for ~2 h to eliminate the surplus of tumor cells.^{17,18} Laser light at 630 nm is used with a light dose of 60 J/cm² and is delivered via a handheld optical fiber that is manually scanned throughout the cavity.¹⁹ The Intralipid in the pleural cavity can be easily pumped out if blood content in the solution is too high to affect light transmission. Dupre et al.²⁰ reported good light-distribution with treatment-averaged fluence rate being very similar among eight detection sites throughout the cavity using ~40-60 mW/cm². The light dosimetry is performed using 8 isotropic detectors.²¹ Intralipid (0.1%) is also used in balloons with optical fibers to address light scattering. In this vein, studies have evaluated light distribution from balloons of different geometries filled with saline or Intralipid solutions.²²

In a study on Intralipid-mediated PDT of three decades ago,¹ PDT with dihematoporphyrin ether of human non-small-cell lung cancer cells (A549) produced high cytotoxicity when cells were maintained in solutions of Intralipid during the illumination. Cell killing was greater in the presence of 1% Intralipid solutions compared to PBS, and evidence suggested that Intralipid promoted the leaching of photosensitizer from the cells. Current PDT studies use dilute solutions of Intralipid (typically 0.01%) for light scattering.

Despite the effectiveness of Intralipid as a light scattering agent in PDT, surprisingly little is known about its stability under sensitized photooxidation conditions. For example, what are the total quenching rate constants (k_T) of $^1\text{O}_2$ with Intralipid and some of its constituents? Can organic phosphines trap Intralipid peroxides formed in photosensitized oxidation reactions?

2 Quenching of singlet oxygen by intralipid

Previous experiments of Gemmell et al.²³ reveal a decrease of $^1\text{O}_2$ luminescence in the presence of Intralipid, which the authors attribute to $^1\text{O}_2$ quenching, or other de-excitation pathways, and/or diffusion of excitation and $^1\text{O}_2$ luminescence at 1270 nm.

This led us to conduct a $^1\text{O}_2$ luminescence study to measure the total quenching rate constants (k_T) of $^1\text{O}_2$ by Intralipid and its constituents. We used a photostable BODIPY sensitizer (Br₂B-OAc), which due to the heavy-atom effect efficiently sensitizes the formation of $^1\text{O}_2$ (Fig. 3).²⁴⁻²⁷ The observed $^1\text{O}_2$ quenching rate constants (k_{obs}) were determined by monitoring the quenching of its time-resolved emission at 1270-1275 nm,^{28,29} in which our k_T data was acquired with a 355 nm pulsed laser light excitation. Water was evaporated from Intralipid leaving behind an oily residue containing mainly a mixture of soybean oil, glycerol, and egg yolk phospholipids. Chloroform was used as the solvent to solubilize this oily residue and also to extend the lifetime of $^1\text{O}_2$ ~70 times to facilitate the k_T measurements. Our measured k_d of ~4280 s⁻¹ is similar to that found in the literature with CHCl₃ as the solvent.³⁰

Data for the three quencher systems, Intralipid (Fig. 4A), a simplified mixture soybean oil (containing only five fatty acids) (Fig. 4B), and oleic acid (containing only a single unsaturated alkene) (Fig. 4C) are shown. Each exponential decay curve is first-order, and the lifetime decrease with increasing concentrations of the quenchers (Fig. 4). The rate of deactivation of $^1\text{O}_2$ by the quenchers was obtained using eqs. 1–3, where Q is the quencher (Intralipid, soybean oil, or oleic acid), k_d is the rate constant for quenching of $^1\text{O}_2$ by the solvent and k_q and k_r are the physical

and chemical quenching rate constants of ${}^1\text{O}_2$ by the quencher, respectively. The sum of k_q and k_r is the total quenching rate constant (k_T).

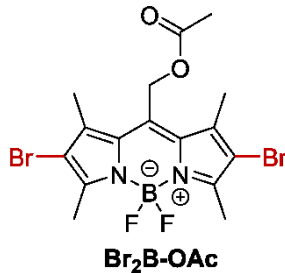


Fig. 3 8-Acetoxyethyl-2,6-dibromo-1,3,5,7-tetramethyl pyrromethene fluoroborate (Br₂B-OAc) was used as a sensitizer in Intralipid, soybean oil, and oleic acid in the ${}^1\text{O}_2$ quenching experiments.

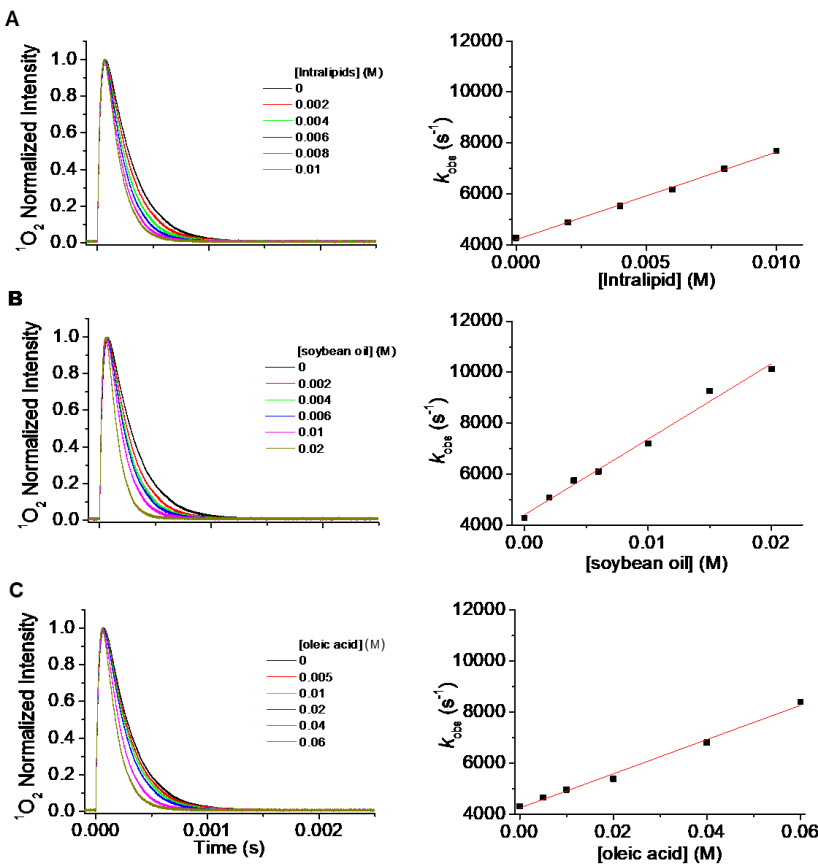


Fig. 4 Normalized ${}^1\text{O}_2$ luminescence decay curves (left column) and total rate constant (k_T) plots (right column) in monitoring the 1270 nm signal in the presence of (A) Intralipid, (B) soybean oil, and (C) oleic acid. Solvent: CHCl_3 at 25 °C.

$$-\frac{d[{}^1\text{O}_2]}{dt} = k_{\text{obs}} [{}^1\text{O}_2] = \{k_d + (k_r + k_q) [Q]\} [{}^1\text{O}_2] \quad (1)$$

$$k_{\text{obs}} = k_d + (k_r + k_q) [Q] \quad (2)$$

$$k_{\text{obs}} = k_{\text{d}} + (k_{\text{T}}) [\text{Q}] \quad (3)$$

Data plotted of k_{obs} vs. [Q] are linear (Fig. 4, right column) from which both the rate constants k_{d} (intercept) and k_{T} (slope) can be determined (Table 1). The highest k_{T} value was found when Intralipid was used as the quencher ($k_{\text{T}} = 3.44 \times 10^5 \text{ M}^{-1} \text{ s}^{-1}$). Intralipid is composed of soybean oil (10%), egg yolk phospholipids (1.2%), glycerol (2.25%), and water. We used a 20% emulsion, which means that upon evaporation of the water, the oily residue is composed of 75% soybean oil, 9% egg yolk phospholipids, and 16% glycerol. Soybean oil itself consists of linoleic acid (44–62%), oleic acid (19–30%), palmitic acid (7–14%), and linolenic acid (4–11%). Even though the amount of soybean oil is less than the 20% emulsion, the increase in the k_{T} value can be attributed to the presence of egg yolk phospholipids and glycerol. Egg yolk phospholipids are at least 70% of phosphatidylcholine. It is known that lipids can have k_{T} values from $1.2 \times 10^{-5} \text{ M}^{-1} \text{ s}^{-1}$ up to $3 \times 10^{-5} \text{ M}^{-1} \text{ s}^{-1}$ depending on the number of unsaturations.³¹ Furthermore, protic molecules, such as glycerol, will also have a contribution to deactivating $^1\text{O}_2$ by physical quenching. The k_{T} for soybean oil ($2.97 \times 10^{-5} \text{ M}^{-1} \text{ s}^{-1}$) is about 5 times higher than the k_{T} for oleic acid ($0.53 \times 10^{-5} \text{ M}^{-1} \text{ s}^{-1}$). This increased k_{T} makes sense based on the composition of these oils. While oleic acid is a monounsaturated lipid, soybean oil has a high percentage of polyunsaturated lipids (44–62%). To illustrate this point, the k_{T} value for linoleic can be up to 2.5 times larger when compared to oleic.³² Thus, in summary for this section, Intralipid as an emulsion, not just the lipids, leads to the quenching of $^1\text{O}_2$.

Table 1. k_{d} and k_{T} measurements for the physical and chemical reaction of solvent and substrate with $^1\text{O}_2$, respectively, in CHCl_3 .

Q	$k_{\text{d}} \times 10^{-3} (\text{s}^{-1})^{\text{a}}$	$k_{\text{T}} \times 10^5 (\text{M}^{-1} \text{ s}^{-1})^{\text{a}}$
oleic acid	4.24 ± 0.09	0.67 ± 0.03
soybean oil	4.41 ± 0.14	2.97 ± 0.14
Intralipid	4.20 ± 0.05	3.44 ± 0.09

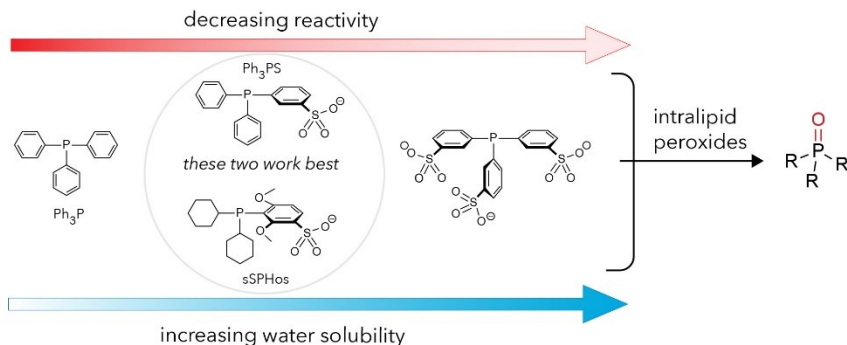
^a Fitting errors reported.

3 Chemical trapping study

To determine whether Intralipid forms peroxides upon photooxidation, a trapping study was carried out using a series of phosphines (Fig. 5).³³ With Al(III) phthalocyanine tetrasulfonic acid chloride (AlPcS) as the sensitizer, trapping of Intralipid peroxides was monitored by oxygen-atom transfer to phosphine traps in the dark following the photooxidation reaction (Fig. 5 and 6).

Our Intralipid peroxide trapping study used a series of phosphines 2'-dicyclohexylphosphino-2,6-dimethoxy-1,1'-biphenyl-3-sulfonate (sSPhos), 3-(diphenylphosphino)benzenesulfonate (Ph₃PS), triphenylphosphine-3,3',3''-trisulfonate (Ph₃PS₃), and triphenylphosphine (Ph₃P). The percent yield of the peroxides increased linearly with the increase in fluence from 45 to 180 J cm^{-2} based on our trapping experiments. This enabled the trapping to quantify the amount of peroxides in the Intralipid photooxidation samples.

The 669-nm light irradiation of AlPcS sensitizer in the presence of Intralipid and O_2 led to the formation of peroxides. The peroxide yields were obtained as a function of light fluence (Table 2). Table 2 shows that the O-atom transfer was dependent more



on the fluence and less on the concentration of the sensitizer. The percent yield of Ph_3PS oxide decreased from 9.3% to 5% with decreasing AlPcS concentration from 100 μM to 10 nM.

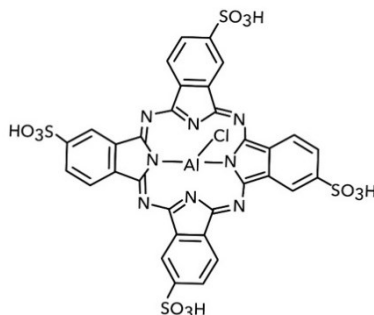


Fig. 5 The four phosphines used in the peroxide trapping studies, which upon oxidation form the corresponding phosphine oxides. The two phosphines highlighted with a circle have a good balance between reactivity and water solubility.

Fig. 6 $\text{Al}(\text{III})$ phthalocyanine tetrasulfonic acid chloride was used as a sensitizer with 669 nm diode laser light in the Intralipid photooxidation experiments, in which the peroxide products were trapped with the organic phosphines.

Table 2. Trapping of peroxides by the organic phosphines from 1% (v/v) Intralipid^a photooxidations

phosphine	potency J/cm^2 (Time)					
	45 ^b (3.75 min)	90 ^b (7.5 min)	135 ^b (11.25 min)	180 ^b (15 min)	90 ^c (7.5 min)	90 ^d (7.5 min)
peroxide yield (%)	sPhos	9 \pm 1.5	10 \pm 1.5	13 \pm 1	18 \pm 1.5	
	Ph ₃ PS	8.3 \pm 1	9.3 \pm 1	13 \pm 1	17 \pm 1	7 \pm 1
	Ph ₃ PS ₃				2	
	Ph ₃ P				-	

^a 1% (v/v) Intralipid = 44 mM; $[\text{AlPcS}] = ^b1 \times 10^{-4} \text{ M}$, $^c1 \times 10^{-6} \text{ M}$ and $^d1 \times 10^{-8} \text{ M}$.

In the series of phosphines, Ph_3PS is the most suitable trapping agent of Intralipid peroxides owing to a balance of nucleophilicity and water solubility. The time required to trap peroxides with phosphines varies from moderate (Ph_3PS) to high (Ph_3PS_3) to low (sSPhos) (Table 3). sSPhos is capable of trapping the peroxy intermediates, but also undergoes air oxidation, thus when used to trap peroxides required a subtraction to account for the extra sSPhos oxide. Ph_3PS_3 is a poor trapping agent due to an electronically deactivated phosphorus site.

Sulfonate groups are water-solubilizing groups, but decreases the nucleophilicity and

oxophilicity. The hydroperoxides are the major products in the Intralipid photooxidation reaction. Dioxetanes can also be formed, but are unstable and consequently decompose to carbonyl fragments during the reaction. Peroxides can also be formed by type I reactions, such as those formed from unconjugated dienes.

A useful facet of this study is that deuterated solvents are not required to monitor the trapping by ^{31}P NMR so that aqueous samples are readily usable. Our work builds on previous reports of phosphine trapping as *in-situ* trapping agents for heteroatom and hydrocarbon peroxides, but in a model reaction for PDT. This study paves the way for the development of Intralipid peroxide quantitation after PDT using phosphine trapping and ^{31}P NMR spectroscopy in H_2O .

Table 3. Phosphine physical and chemical properties

phosphine	physical property		chemical properties	
	solubility	stability of commercial sample	Reaction with hydroperoxides	
sSPhos	Water soluble on heating to 40 °C (100 mg/L) ^a	7% oxide impurity, quality decreased over time		instantly
Ph_3PS	water soluble above RT (100 mg/L) ^a	no oxide impurity		within minutes
Ph_3PS_3	water soluble at RT (100 mg/L) ^a soluble in organic solvents (50 mg/mL, CHCl_3) ^b	5% oxide impurity	after 12 h, reaction is incomplete	
Ph_3P		no oxide impurity		instantly

^a Values adapted from reference 33; ^b Reported in compound specification sheet (Aldrich).

4 Conclusion

Instead of being unreactive, some constituents of Intralipid are able to interact with ROS formed in sensitized photooxidations. This raises a possibility for photooxidation reactions with Intralipid by $^1\text{O}_2$ 'ene' reactions and [2 + 2] cycloadditions, and also type I reactions (Fig. 7). Key questions that remain are what are the relative concentrations of Intralipid peroxides and whether their lifetimes vary significantly.

Of note, Cadet and others,⁷ suggest that PDT is usually 75% $^1\text{O}_2$ and 25% type I. Typical sensitizers act mainly through the type II process,³⁻⁷ although taking into account the fact that association, such as methylene blue with DNA, offers a route to type I processes.^{3-7,34,35} A number of amine-substituted sensitizers seem also to be controlled by type I processes due to patterns of oxidation (e.g., $\text{R}_2\text{N}^{\cdot+}$ to radical cations) and/or demethylation (e.g., methylene blue and toluidine blue).³⁶

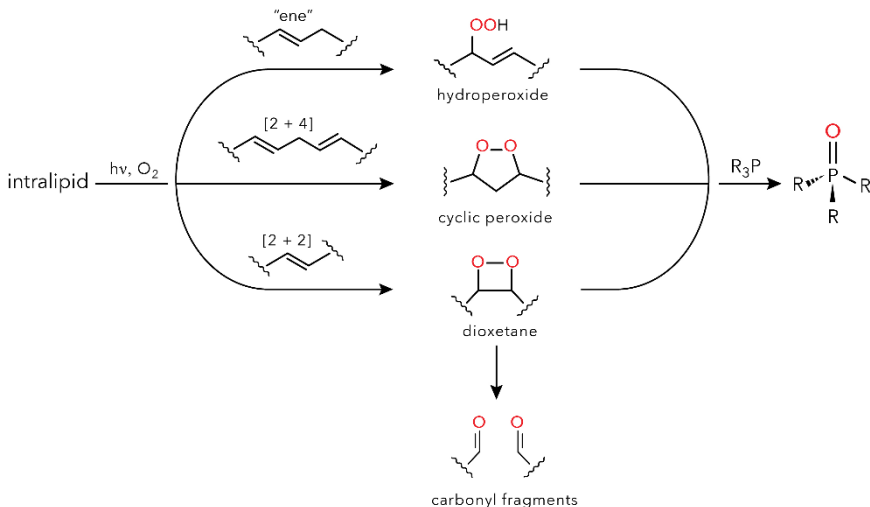


Fig. 7 Photooxidation of Intralipid to form transient peroxide products trapped by phosphines (R_3P) to form phosphine oxides ($R_3P=O$).

5 Prospectives

A Step Closer to Intralipid's Role in Photodynamic Therapy

If the Intralipid peroxides are unstable, how might they perturb pleural PDT, by their oxidative character? Intralipid peroxides could be tested for toxicity to cells, such as breast cancer cells using photoaged Intralipid samples. The answer could lie in treating cells that are bathed in Intralipid and followed for survival. The intention would be to introduce delays between PDT of Intralipid and the exposure of the cells to the Intralipid. In this way, location could be varied intracellularly and extracellularly to learn of toxicity effects of endogenous and exogenous Intralipid peroxides from sensitized photooxidations.

Acknowledgement

A.M.D., P.P.M., M.A., M.E.Z., and A.G. acknowledge support from the National Science Foundation (CHE-1856765). A.M.D. also acknowledges support from a Fulbright-CONICET fellowship. M.M.K., K.A.C., T.C.Z. and T.M.B. acknowledge the support from the National Institutes of Health (NIH) R01 CA236362, R01 CA154562, and/or P01 CA87971. We thank Leda Lee for the graphic arts work.

References

- ^aDepartment of Chemistry, Brooklyn College, Brooklyn, NY
- ^bPh.D. Program in Chemistry, The Graduate Center of the City University of New York, New York, NY
- ^cIDAS-CONICET, Departamento de Química, Facultad de Ciencias Exactas, Físico-Químicas y Naturales, Universidad Nacional de Río Cuarto, Río Cuarto, Córdoba, Argentina
- ^dDepartment of Radiation Oncology, University of Pennsylvania, Perelman Center for Advanced Medicine, Philadelphia, PA

1. R. R. Perry, S. Evans, W. Matthews, W. Rizzoni, A. Russo and H. I. Pass, *J. Surg. Res.*, 1989, **46**, 386-390.
2. F. Aziz, S. Telara, H. Moseley, C. Goodman, P. Manthri and M. S. Eljamal, *Photodiagn. Photodyn.*, 2009, **6**, 227-230.
3. M. S. Baptista, J. Cadet, P. Di Mascio, A. A. Ghogare, A. Greer, M. R. Hamblin, C. Lorente, S. C. Nunez, M. S. Ribeiro, A. H. Thomas, M. Vignoni and T. M. Yoshimura, *Photochem. Photobiol.*, 2017, **93**, 912-919.
4. C. S. Foote, *Photochem. Photobiol.*, 1991, **54**, 659-659.
5. (a) Y. H. Ong, A. Dimofte, M. M. Kim, J. C. Finlay, T. Sheng, S. Singhal, K. A. Cengel, A. G. Yodh, T. M. Busch, T. C. Zhu, *Photochem. Photobiol.* 2020, **96**, 340-348. (b) A. Greer, *Acc. Chem. Res.*, 2006, **39**, 797-804.
6. J. P. Celli, B. Q. Spring, I. Rizvi, C. L. Evans, K. S. Samkoe, S. Verma, B. W. Pogue, T. Hasan, *Chem. Rev.*, 2010, **110**, 2795-2838.
7. J. Cadet, C. Decarroz, S. Wang and W. Midden, *Isr. J. Chem.*, 1983, **23**, 420-429
8. M. M. Kim, A. A. Ghogare, A. Greer, T. C. Zhu, *Phys. Med. Biol.*, 2017, **62**, R1-R48.
9. (a) A. W. Girotti, *J. Photochem. Photobiol. B*, 2001, **63**, 103-113. (b) M. Niziolek, W. Korytowski, A. W. Girotti, *Photochem. Photobiol.*, 2005, **81**, 299-305.
10. (a) E. L. Clennan, A. Pace, *Tetrahedron*, 2005, **61**, 6665-6691. (b) E. L. Clennan, *Molecular and Supramolecular Photochemistry*, 2005, **12**, 365-390.
11. (a) S. Protti, M. Fagnoni, A. Albini, Edited by W. Zhang, B. W. Cue, *Green Techniques for Organic Synthesis and Medicinal Chemistry* (2nd Ed.), 2018, 373-406. (b) D. Ravelli, S. Protti, P. Neri, M. Fagnoni, A. Albini, *Green Chem.*, 2011, **13**, 1876-1884.
12. (a) A. G. Griesbeck, Edited by W. M. Horspool, P.-S. Song, *CRC Handbook of Organic Photochemistry and Photobiology*, 1995, 301-310. (b) A. G. Griesbeck, M. Kleczka, A. de Kiff, M. Vollmer, A. Eske, S. Sillner, *Pure Appl. Chem.*, 2015, **87**, 639-647.
13. W. Fudickar, T. Linker, *Aust. J. Chem.* 2014, **67**, 320-327.
14. (a) M. N. Alberti and M. Orfanopoulos, *Chem. Eur. J.*, 2010, **16**, 9414-9421. (b) M. N. Alberti and M. Orfanopoulos, *Synlett*, 2010, **7**, 999-1026. (c) M. Orfanopoulos, C. S. Foote, *J. Am. Chem. Soc.*, 1988, **110**, 6583-6584.
15. C. Munck, S. R. Mordon, A. Scherpereel, H. Porte, X. Dhalluin and N. Betrouni, *Ann. Thorac. Surg.*, 2015, **99**, 2237-2245.
16. J. S. Friedberg, M. J. Culligan, R. Mick, J. Stevenson, S. M. Hahn, D. Sterman, S. Punekar, E. Glatstein and K. Cengel, *Ann. Thorac. Surg.*, 2012, **93**, 1658-1667.
17. S. K. Hendren, S. M. Hahn, F. R. Spitz, T. W. Bauer, S. C. Rubin, T. C. Zhu, E. Glatstein and D. L. Fraker, *Ann. Surg. Oncol.*, 2001, **8**, 65-71.
18. T. W. Bauer, S. M. Hahn, F. R. Spitz, A. Kachur, E. Glatstein and D. L. Fraker, *Ann. Surg. Oncol.*, 2001, **8**, 254-259.
19. J. S. Friedberg, R. Mick, J. P. Stevenson, T. Zhu, T. M. Busch, D. Shin, D. Smith, M. Culligan, A. Dimofte, E. Glatstein and S. M. Hahn, *J. Clin. Oncol.*, 2004, **22**, 2192-2201.
20. P. J. Dupre, Y. H. Ong, J. Friedberg, S. Singhal, S. Carter, C. B. Simone, 2nd, J. C. Finlay, T. C. Zhu, K. A. Cengel and T. M. Busch, *Photochem. Photobiol.*, 2020, **96**, 417-425.
21. A. D. Dimofte, T. C. Zhu, J. C. Finlay, M. Cullingham, C. E. Edmonds, J.S . Friedberg, K. Cengel, S. M. Hahn, *Proc. SPIE*, 2009, 7164.
22. H. Moseley, C. McLean, S. Hockaday and S. Eljamal, *Photodiagn. Photodyn.*, 2007, **4**, 213-220.
23. N. R. Gemmell, A. McCarthy, M. M. Kim, I. Veilleux, T. C. Zhu, G. S. Buller, B. C. Wilson and R. H. Hadfield, *J. Biophotonics*, 2017, **10**, 320-326.
24. M. L. Agazzi, J. E. Durantini, N. S. Gsponer, A. M. Durantini, S. G. Bertolotti, E. N. Durantini, *ChemPhysChem*, 2019, **20**, 1110-1125.
25. A. M. Durantini, D. A. Heredia, J. E. Durantini, E. N. Durantini, *Eur. J. Med. Chem.* 2018, **144**, 651-661.
26. R. Lincoln, A. M. Durantini, L. E. Greene, S. R. Martinez, R. Knox, M. C. Becerra and G. Cosa, *Photochem. Photobiol. Sci.*, 2017, **16**, 178-184.
27. A. M. Durantini, L. E. Greene, R. Lincoln, S. R. Martinez, G. Cosa, *J. Am. Chem. Soc.* 2016, **138**, 1215-1225.
28. S. Nonell and C. Flors, in *Singlet Oxygen: Applications in Biosciences and Nanosciences, Volume 2*, The Royal Society of Chemistry, 2016, vol. 2, pp. 1-6.
29. J. C. Schlothauer, M. Pfitzner and B. Röder, in *Singlet Oxygen: Applications in Biosciences and Nanosciences, Volume 2*, The Royal Society of Chemistry, 2016, vol. 2, pp. 43-62.
30. J. R. Hurst, J. D. McDonald and G. B. Schuster, *J. Am. Chem. Soc.*, 1982, **104**, 2065-2067.

31. A. A. Krasnovsky, V. E. Kagan and A. A. Minin, *FEBS Lett.*, 1983, **155**, 233-236.
32. C. Vever-Bizet, M. Dellinger, D. Brault, M. Rougee and R. V. Bensasson, *Photochem. Photobiol.*, 1989, **50**, 321-325.
33. P. P. Mohapatra, C. O. Chiemezie, A. Kligman, M. M. Kim, T. M. Busch, T. C. Zhu and A. Greer, *Photochem. Photobiol.*, 2017, **93**, 1430-1438.
34. A. A. Ghogare and A. Greer, *Chem. Rev.*, 2016, **116**, 9994-10034.
35. W. Adam, C. Saha-Moeller, A. Schoenberger, M. Berger and J. Cadet, *Photochem. Photobiol.*, 1995, **62**, 231-238.
36. J. Robinson-Duggon, N. Mariño-Ocampo, P. Barrias, D. Zúñiga-Núñez, G. Günther, A. M. Edwards, A. Greer and D. Fuentealba, *J. Phys. Chem. A*, 2019, **123**, 4863-4872.